CONDUITS AND TURBULENT FLOW IN THE EDWARDS AQUIFER

Prepared for:

EDWARDS AQUIFER AUTHORITY
San Antonio, Texas

December 20, 2003

Prepared by:

Stephen R. H. Worthington
Worthington Groundwater
55 Mayfair Avenue
Dundas, Ontario, Canada

Conduits and turbulent flow in the Edwards Aquifer

Stephen R.H. Worthington

1 Introduction

Over the period 2000-2003 the US Geological Survey developed a new numerical model to simulate flow in the San Antonio segment of the Edwards Aquifer. In the early stages of this process the question arose as how to best incorporate into the model the high permeability found in some areas of the aquifer. It has generally been recognized that the high permeability in the Edwards Aquifer is due to dissolution of the limestone bedrock (Maclay, 1995), and Halihan et al. (2000) concluded that "conduits ... control regional-scale permeabilities and have turbulent flow" (Halihan et al., 2000, p. 129). If the location and characteristics of conduits could be either predicted on theoretical evidence or determined from aquifer measurements then this would offer the possibility of incorporating the conduits into the model and thereby produce a more accurate representation of the aquifer. This would be especially true if the conduits are organized into an aquifer-scale network. On the other hand the possibility was raised that conduits might only be local features, and that the aquifer might behave like a porous medium at a large scale. This raised three important questions:

a) What are the characteristics of aquifer-scale conduit networks?
b) What tests can be applied to determine whether there are aquifer-scale conduit networks in the Edwards Aquifer?
c) where might such conduit networks be located and how could they be incorporated in the USGS numerical model?

These three questions are addressed in sections 2, 3, and 4, respectively.

2 Characteristics of aquifer-scale conduit networks

The presence of an integrated aquifer-wide network of solutionally-enlarged conduits with rapid flow is the key property of karst aquifers (Huntoon, 1995; Worthington, 1999). These networks form tributary systems that discharge at springs. This fundamental concept is supported by both empirical and theoretical evidence.

Tracer testing provides the major evidence for extensive conduits in carbonate aquifers. The first aquifer-scale test took place in 1877, with a trace from sinkholes in the bed of the Danube River. The traced water crossed the European continental divide to emerge 12 km away at a spring feeding one of the headwaters of the Rhine River, the other major river in Europe. The travel time was just two days, and the calculated Reynolds number is about 500,000. Flow was clearly in the turbulent regime over this 12 km distance.

By the turn of the century dozens of similar tests had been performed (Dole, 1906) and the total now exceeds ten thousand. The average velocity along conduits is 1700 m/day, based on a representative set of 2877 tracer tests (Worthington et al., 2000a). The mean distance traced in this data set was 6.3 km, and 124 traces were over distances of at least 20 km. Calculated Reynolds numbers for these very long distance traces almost always exceed 100,000, demonstrating the scale to which conduit networks with turbulent flow extend.

Hydrogeological studies within caves provide a useful supplement to this tracing data for studying conduit characteristics and flow and dissolution processes. Mapping of caves is approximately doubling the total length of known caves each decade, but the longest distance a cave stream has been followed is only 19 km. Such streams usually descend below the water table, where scuba exploration of these conduits is extremely difficult and dangerous, so relatively few water-filled conduits have been explored. Thus cave maps only show a small fraction of the actual conduit flow that occurs within an aquifer. Investigations of different well testing and monitoring methods for inferring karstification have shown that the probably of a randomly drilled well intersecting a major conduit in a karst aquifer is only about 2% (Worthington et al., 2000b). The remaining 98-99% of wells intersect the rock matrix and fractures and possibly small conduits.

The theory of karst conduit formation greatly lagged behind the field evidence, and only in the last thirty years has a satisfactory theoretical basis been developed. The first critical development was the investigation of the dissolution kinetics of limestone in a series of laboratory experiments, starting in the 1970s (Berner and Morse, 1974; Plummer and Wigley, 1976). The second critical development involved the use of numerical modeling to simulate the development of conduits by coupling kinetic and equilibrium dissolution with aquifer hydraulics. Understanding rapidly advanced in the 1990s, and Dreybrodt (1996) showed that the development of conduits was to be expected in all limestone aquifers where there is ready

recharge and discharge. Worthington (2001) showed that conduit development deep below the water table is favored where flow paths are longer than 3 km.

3 Tests for aquifer-scale conduit networks

3.1 Local-scale tests for aquifer-scale conduit networks

Worthington and Ford (1997) and Worthington (1999) summarize a number of well tests that may be used to assess karstification in a limestone aquifer. However, the problem with any well testing or monitoring is that there is little evidence whether the enhanced flow commonly found at certain horizons in a well is only of local scale or whether it is more extensive. One major indication of karstification in an aquifer is large and rapid changes in water levels and spring discharges following rainfall. The major rainfall event in October 1998 provides a good example of the rapidity and the range of the response of the Edwards Aquifer to rain.

The intense rainfall of October 17-19 1998 was centered on Comal County, with more than 20 inches being recorded at Bulverde and New Braunfels, and 15 inches at San Antonio airport. Rainfall diminished to the west, with 10 to 11 inches being recorded in Medina County and 2 to 4 inches in Uvalde County. The response in the aquifer recharge zone in Bexar County to this rain is shown in Figure 1. The median lag between rainfall and maximum water level was 60 days, but there is much variability. For instance, the water level at the NAWQA Driving Range well on Blanco Road had risen 134 feet by October 20th, and thereafter was in recession. At the other extreme the water level in the well at Lockhill Selma rose only 24 feet and did not reach its peak until February 1999.

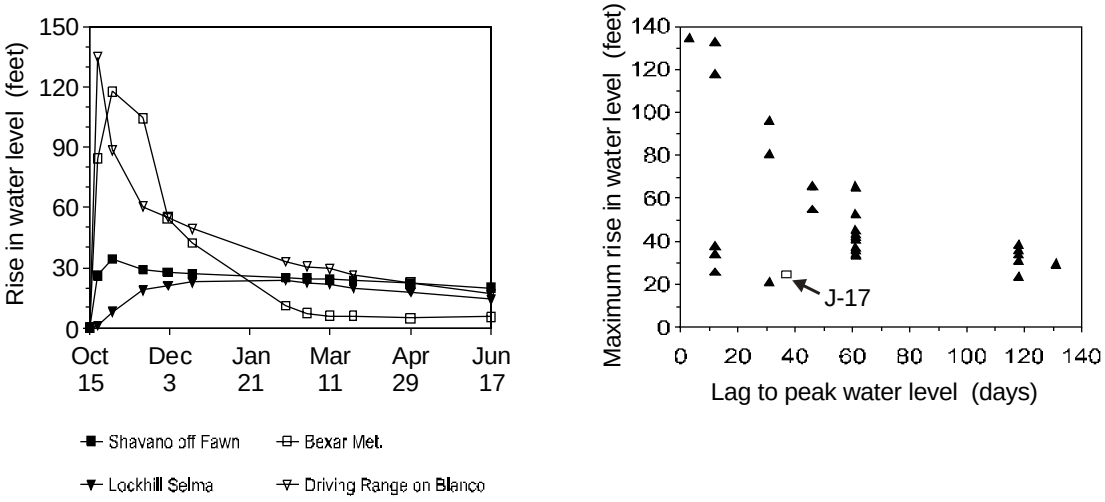

Figure 1 Rise in water level in Bexar County recharge zone following the October 1998 storm, base on USGS water level measurements. Changes in water level over time in four wells in the Shavano Park area (left), and water level rises in all the wells studied as a function of lag to peak water level (right).

The early response at Comal and San Marcos Springs to the October 1998 rainfall is unknown since both gauges also record the flow of intermittent surface creeks (Figure 2). Following the large flows during and after the rainstorm, these creeks stopped flowing on October 26th at San Marcos and on October 28th at Comal Springs. After this time both springs were in recession, showing that the maximum lag between rainfall and peak spring flow was nine days or less at San Marcos Springs, and 11 days or less at Comal Springs. However, the effects of watering restrictions in San Antonio in August 2000 give an indication of the rapidity of spring response (personal communication, Geary Schindel). During a three-week period in August 2000 the water level at J-17 dropped from 643 feet to 640 feet. However, water levels rose on each Saturday and Sunday during this period (Figure 3). At Comal Springs there was either a lessening in the decrease in discharge or an actual increase beginning on each Saturday, showing that the lag between a change in water levels in San Antonio and a response at Comal Springs occurs in less than one day. Similarly, the response at Hondo was almost as rapid (Figure 3).

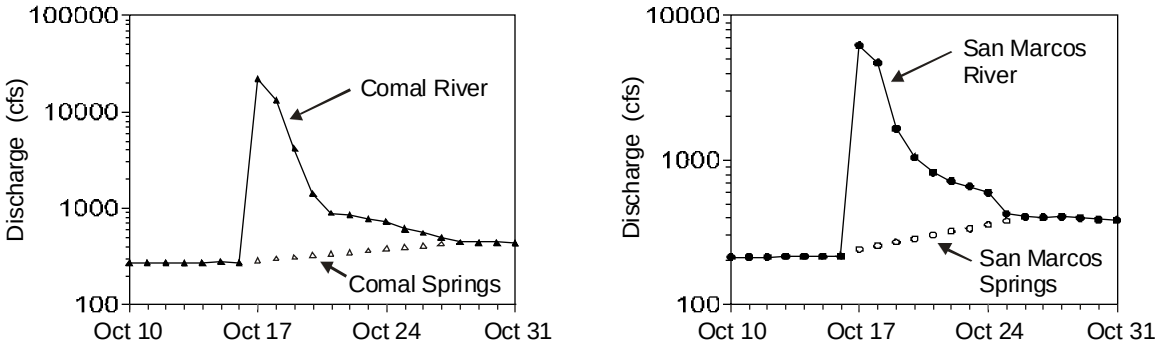

Figure 2 Discharges from Comal River and San Marcos River in 1998, showing the interpolated estimates of spring flow while surface creeks were flowing off the recharge zone (after USGS data).

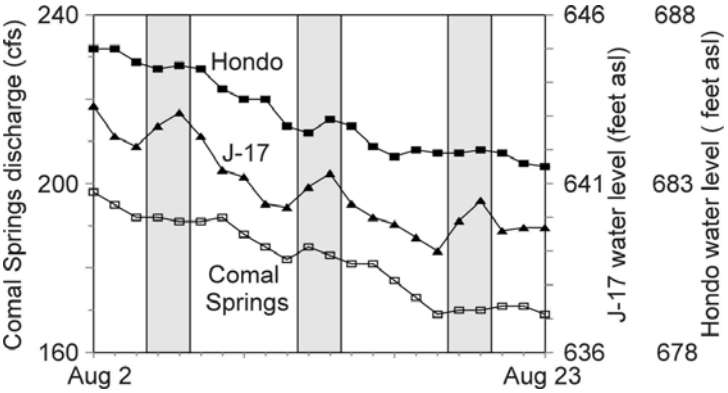

Figure 3 Water level changes in the Medina County (Hondo) and Bexar County (J-17) index wells and discharge changes at Comal Springs in August 2000, showing the effect of watering restrictions on weekends (shaded area on chart).

The median lag to peak water level of eight wells in the confined aquifer is 64 days. Well J-17 reached a maximum after 37 days, and was the most responsive of the eight confined aquifer wells studied by Tomasko et al. (2001). However, half the rise of 24 feet at J-17 occurred between October 17th and October 19th, and a third of the rise of 27 feet at the Hondo well occurred between October 18th and October 20th. Water levels and spring discharges showed a general downward trend through most of 1999 (Figure 4). The recessions at Comal Springs and San Marcos Springs approximate exponential recessions, which are shown in Figure 4 by dashed lines. However, there are some deviations from this, such as during November 1998 at San Marcos Springs, following heavy rain (e.g. 5.8 inches at Wimberley), and in July 1999 when rain affected both springs. Despite the large volumes of water recharged to the aquifer, the average storage time at Comal Springs and San Marcos Springs was only 112 days and 42 days, respectively (Table 1).

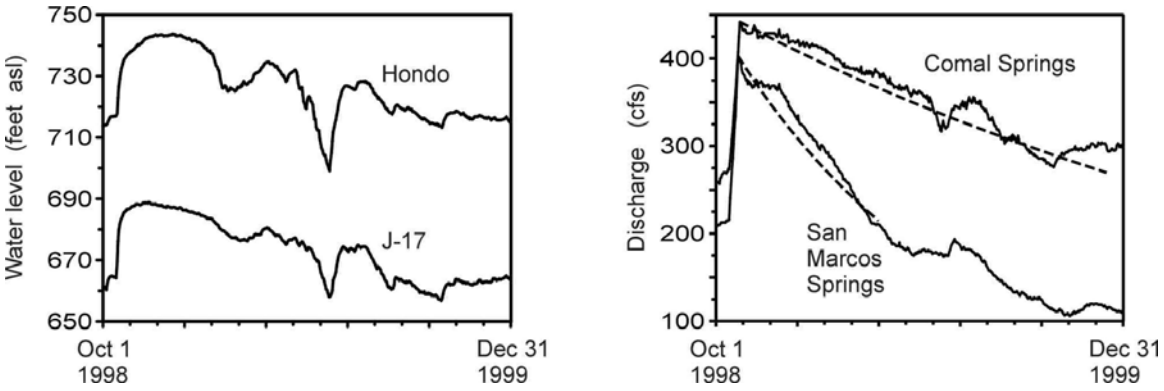

Figure 4 Changes following the October 1998 storm in water levels at the Medina County and Bexar County index wells (left) and at the major springs (right)

Table 1 Characteristics of the recession at Comal and San Marcos Springs

Characteristic	Comal Springs	San Marcos Springs
Maximum discharge (cfs)	442	403
Exponential recession, Q(t)=	442 exp(-0.0012t)	403 exp(-0.004t)
Pre-storm discharge (cfs)	270	215
Time to return to pre-storm discharge (days)	411	157
Median storage time (days)	112	42

The above data from a single storm demonstrate two distinct responses in the aquifer. A few wells in the recharge zone together with Comal and San Marcos Springs show a rapid and large response, with peak levels being reached within a few days of the storm. The peak responses in the springs are driven by high heads in the conduits that feed the springs, with the pressure pulse from the increased water levels in the recharge zone being transmitted quickly to the springs. Conversely, most wells show a much slower and smaller response, with peak water levels being attained after about two months. These wells are not located on conduits and their response is attenuated by the much lower permeability in the matrix and smaller fractures in the aquifer.

3.2 Aquifer-scale tests for aquifer-scale channel networks

Tracer tests are the standard method to demonstrate large-scale channel networks in limestone aquifers where sinking streams and springs are both found, but these are difficult to apply in the Edwards Aquifer due to the large well abstractions in San Antonio and the exceptional scale of the aquifer. An alternative method involves identifying aquifer characteristics that differ between a karst aquifer and an ideal porous medium and to compare the Edwards to these two end-members.

Mammoth Cave is the most extensive known cave in the world, and has been the subject of many karst studies, including two books on the geology and hydrogeology of the area (Palmer, 1981; White and White, 1989). The best-characterized portion of the aquifer is the groundwater basin draining to Turnhole Springs (Quinlan et al., 1986; Hess and White, 1988; Worthington et al., 2000a; Worthington, 2003). This groundwater basin is used as the type example of an ideal well-karstified carbonate aquifer. Figure 5 shows the difference in water-table configuration between this type example of a karst aquifer and an ideal (i.e. homogeneous and isotropic) porous medium aquifer such as in sand. Table 2 lists six major differences between these two aquifer types. These six criteria are applied below to the Edwards Aquifer.

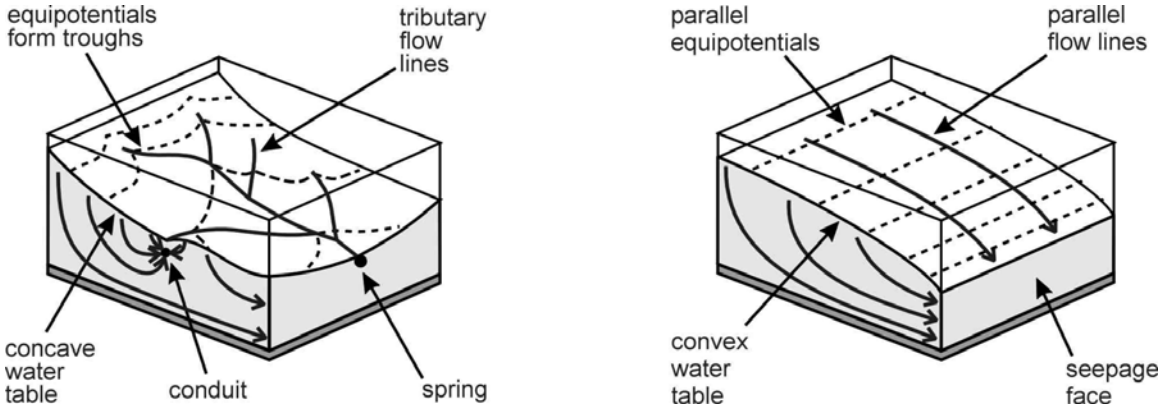

Figure 5 Block diagrams to show the major differences between an ideal carbonate aquifer (left) and an ideal sand aquifer (right)

Table 2 Major aquifer-scale differences between the Turnhole Spring karst aquifer and an ideal sand aquifer

#	Criterion	Karst aquifer	Sand aquifer	Test method
1	discharge to surface	convergent flow to springs	parallel flow lines to seepage face	check for presence of springs or seepage faces
2	shape of potentiometric surface (normal to major flow lines)	equipotentials form troughs	equipotentials are parallel	plot potentiometric surface from heads in wells
3	downgradient trend in hydraulic gradient	decreases	increases	plot potentiometric surface from heads in wells
4	downgradient trend in hydraulic conductivity	increases	no change	calculate change in hydraulic conductivity
5	scaling effects	substantial	none	compare hydraulic conductivity from different scales
6	flow regime	laminar in matrix and fractures, turbulent in conduits	laminar	a) tracer tests to springs b) regress spring discharge against head in wells

Nature of discharge to the surface from the Edwards Aquifer

The discharge from the Edwards Aquifer to the surface occurs at six groups of springs, with Comal Springs, San Marcos Springs and Hueco Springs accounting for more than 90% of the total spring discharge, which in 1997-2002 averaged 640 cfs. These springs all have multiple orifices and all occur on or close to major faults. Multiple orifices are common for springs in

karst aquifers (Quinlan and Ewers, 1989). All the spring orifices at San Marcos Springs and the majority of the spring orifices at Comal Springs emerge from the bottom of artificial lakes. There is usually no surface flow into these lakes, but following major rainstorms ephemeral creeks (Sink Creek at San Marcos Springs and Blieders Creek at Comal Springs) feed these lakes and deposit fluvial sediments onto the lake bottoms. These deposits may have resulted in an increased number of spring orifices in the lake bottoms.

Shape of the potentiometric surface (normal to major flow lines to the springs)

There are steep hydraulic gradients from the unconfined aquifer to the confined aquifer. Within the confined aquifer pronounced troughs in the potentiometric surface are found in a number of places, suggesting that there are major high-permeability conduits. The best two examples are shown in Figure 6.

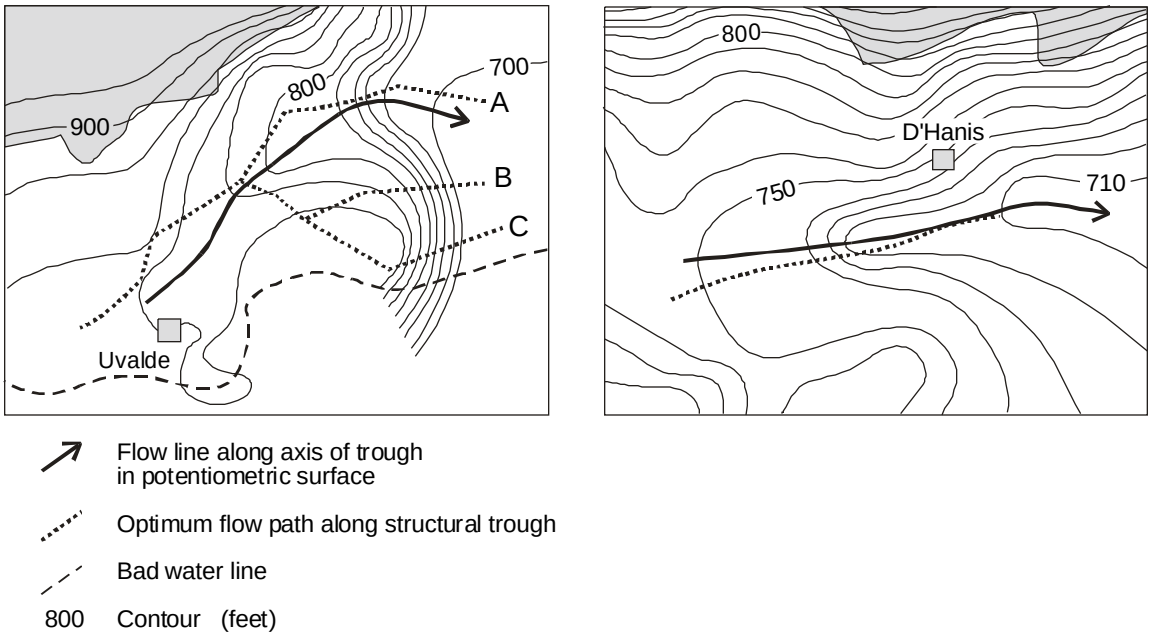

Figure 6 Coincidence of structural and potentiometric surface troughs near Uvalde (left) and near D'Hanis (right), based on structural data from Collins and Hovorka (1997) and on water-level data from Welder and Reeves (1964) and Klemt et al. (1979)

Downgradient trend in hydraulic gradients

Hydraulic gradients along the major flow lines to the two major springs are shown in Figure 7. In both cases the profiles are concave as is typical of karst aquifers. The steep hydraulic gradients 75 km along the flow path to Comal Springs are probably due to extensive intrusives in Uvalde County.

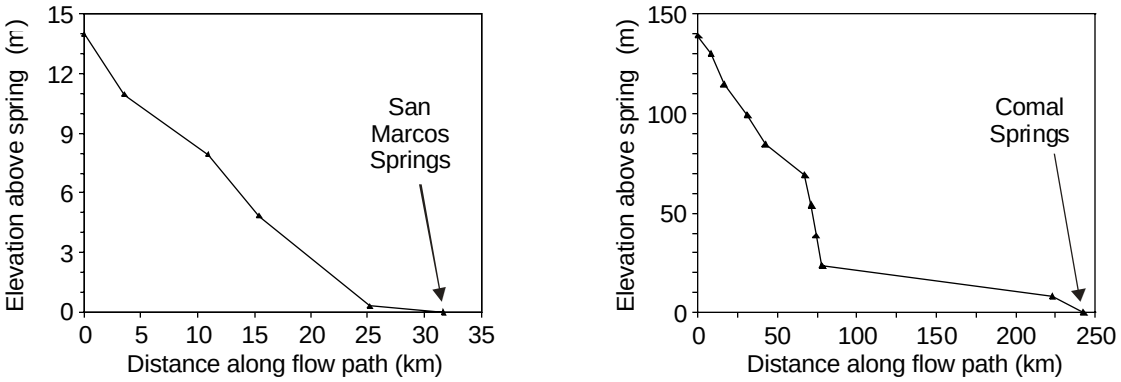

Figure 7 Elevations in the potentiometric surface along major flow paths to San Marcos Springs (left) and to Comal Springs (right) based on water levels in Klemt et al. (1979), Ogden et al. (1986) and Maclay (1995).

Downgradient trends in hydraulic conductivity

Figure 8 shows the trend in hydraulic conductivity (*K*) along the major flow path to Comal Springs in the GWSIM model (Klemt et al., 1979; Thorkildsen and McElhaney, 1992). There is a marked increase in a downgradient direction, suggesting that conduits increase in size and/or number as the springs are approached.

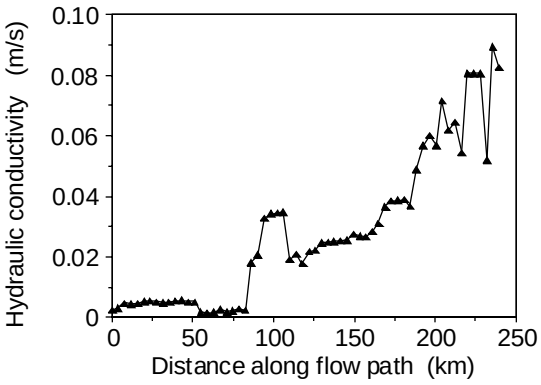

Figure 8 Trend in hydraulic conductivity in the GWSIM model along the flow path from the Brackettville divide to Comal Springs

Scaling effects in hydraulic conductivity

In a porous medium the geometric mean *K* derived from pumping tests can be used for aquifer simulations. This is not the case in the Edwards Aquifer, where there is a pronounced scaling effect and much higher values are needed to simulate spring flow (Halihan et al., 1999, 2000). Figure 9 shows the ratio between the *K* values used in GWSIM (Klemt et al., 1979) and the *K* values derived from kriging of well pumping test data (Hovorka et al., 1998). *K* values in the models are more than 100 times higher than pumping test values over much of the confined aquifer. This shows that the pumping test values are not representative of aquifer permeability, and suggests that there is a high-permeability conduit network that few wells intercept. A rare well that does appear to intercept a major conduit is the Living Waters Well in southern Bexar County, where 37,000 gpm flowed from an 85 ft open interval in a 28-inch well. Swanson (1991) suggested that this is the world's most productive water well.

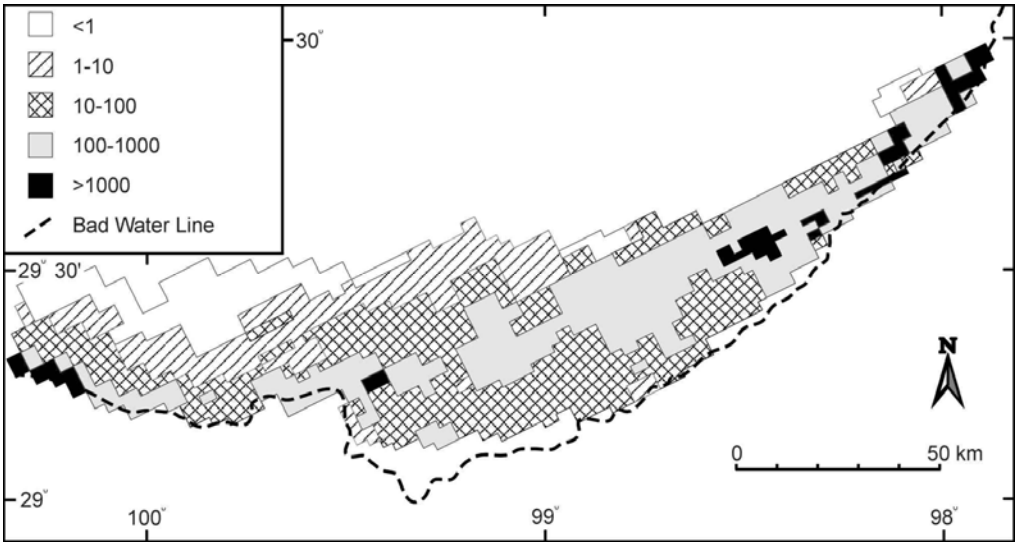

Figure 9 Ratio of the transmissivity values used in the GWSIM model (Klemt et al., 1979) to those derived from kriging of well pumping tests (Hovorka et al., 1998)

Figure 10 shows a comparison between two aquifer simulations (Klemt et al., 1979; Maclay and Land, 1988) and a recent geostatistical analysis of the pumping test data (Painter, personal communication, 2001). The two model simulations have very similar *K* distributions, and the geostatistical analysis is similar at low K values. However, there is a large discrepancy at high *K* values, again indicating that the pumping tests data fails to represent the high-*K* conduits.

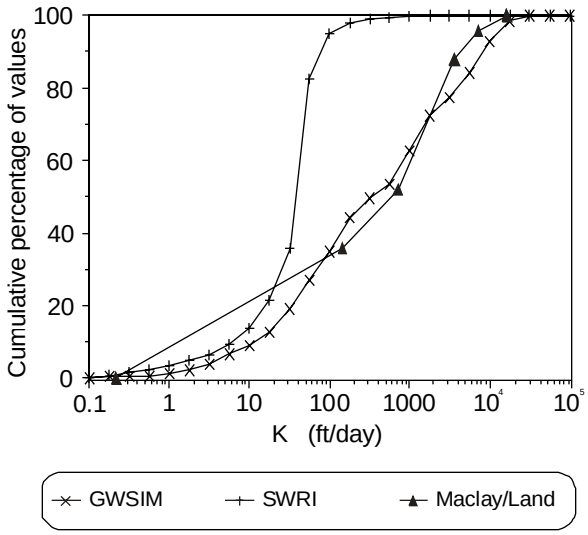

Figure 10 Hydraulic conductivity for the Edwards aquifer used in the GWSIM model (Klemt et al., 1979), the USGS model (Maclay and Land, 1988), and derived from a geostatistical analysis of pumping test data (Scott Painter, personal communication, 2001)

Comparison between the Edwards Aquifer and other karst aquifers shows that the scaling effect is similar (Figure 11). The implication is that the Edwards is similarly karstified to other karst aquifers and thus has a well-developed conduit network.

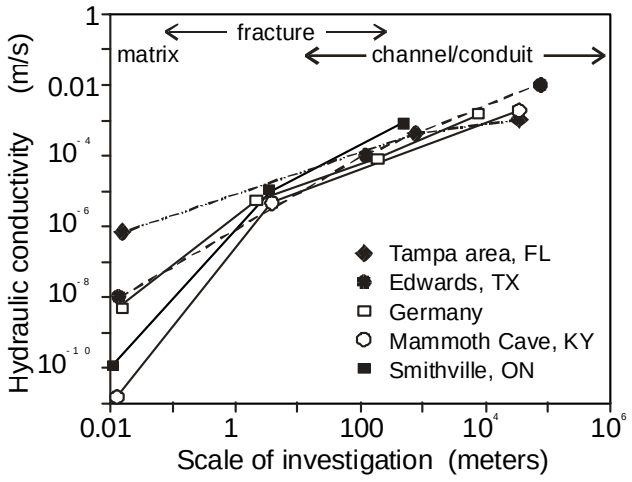

Figure 11 Scaling in hydraulic conductivity in the Edwards Aquifer and in other karst aquifers (after Worthington et al., 2002).

Flow regime

Atkinson and Smart (1981) suggested that the presence of turbulent flow in conduits is the definitive characteristic of karst aquifers. However, the probability of a randomly drilled well intersecting a conduit is only about 0.02 (Worthington et al., 2000b), and so single-well tests are rarely able to identify if conduits with turbulent flow are present in an aquifer. However, tests involving multiple wells or wells and springs offer better methods for testing for turbulent flow. Tracer tests and head differences between wells and springs are two such methods.

The presence of major springs makes the Edwards an ideal aquifer to carry out tracer tests since flow paths converge on these springs and thus natural gradient tests can be used with a small number of sampling points. Comprehensive testing has taken place in the Barton Springs segment of the aquifer, where 17 successful traces have been carried over distances up to 29 km (Hauwert et al, 2002a, 2002b). Other tests in the Edwards Aquifer over distances up to several kilometers have been carried out by Ogden et al. (1986), Rothermel and Ogden (1987), Maclay et al. (1981), Schindel (2002), and Schindel et al. (2002). Table 3 shows the longest successful traces to each of the four major springs.

Table 3 Tracer test results for four major springs in the Edwards aquifer

	Comal Springs	San Marcos Springs	Hueco Springs	Barton Springs
Injection point	LCRA well	Ezell's Cave	Blieders Creek	Crooked Oak Cave
Distance	0.8 km	3.3 km	4 km	29 km
Spring discharge	180*	50*	80	29
Tracer velocity	240 m/day	180 m/day	800 m/day	1200 m/day
Reynolds number	140,000	64,000	170,000	130,000
Reference	Schindel et al. (2002)	Ogden et al. (1986), Schindel (2002)	Rothermel and Ogden (1987)	Hauwert et al. (2002a)

* The tracer did not emerge from all spring orifices. Discharges used are estimates of the total discharge from the orifices from which the tracer emerged.

A second method of identifying turbulent flow is to compare the relationship between spring discharge and the head in wells. Head changes are proportional to specific discharge if flow is laminar, but change with the square of discharge if flow is turbulent (Street et al., 1996, p. 232). This can be expressed as

$$< = -K\ i^m \quad (1)$$

where < is the specific discharge, *K* is hydraulic conductivity, i is the hydraulic gradient, and m is an exponent which depends on the flow regime (Freeze and Cherry, 1989, p. 72). The exponent m ranges from 0.5 for turbulent flow to 1 for laminar flow.

If a well intercepts a conduit, if the conduit is flooded for its entire length to a spring, and if there is turbulent flow in the conduit, then exponent m in Equation 1 will have a value of 0.5. It is very unlikely for a well to intercept a major conduit, but wells frequently intercept open, transmissive fractures, in which the flow regime is laminar. Such fractures may be well connected to major conduits, resulting in exponent m being between 0.5 and 1, reflecting in part the laminar flow in the fracture and in part the turbulent flow in the conduit.

Figure 12 shows head and spring discharge correlations between Barton Springs and a well located 4 km to the south which is close to a trough in the potentiometric surface. The major conduit feeding Barton Springs is inferred to be associated with this trough, and turbulent flow in the conduit has been established by tracer testing such as the trace from Crooked Oak Cave to Barton Springs (Table 3). There is a high correlation between head in Well YD-58-50-216 and spring discharge, which indicates a good hydraulic connection. The exponent of head in the regression equation is very close to the 0.5 value in Equation 1, indicating that there is turbulent flow along the flow path between the well and the spring. Recent tracer testing between a number of sinking streams and Barton Springs have demonstrated groundwater velocities of 1 - 6 km/day, confirming that turbulent flow in conduits occurs along a number of pathways in the aquifer (Hauwert et al., 2002a, 2002b)

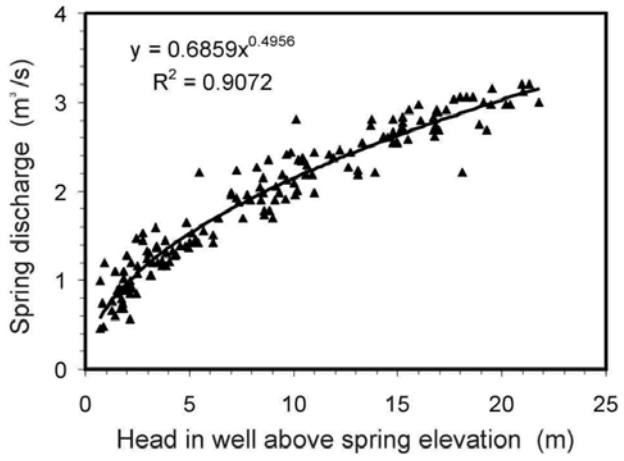

Figure 12 Correlation between head in well YD-58-50-216 and discharge at Barton Springs, demonstrating turbulent flow in the aquifer (data from Texas Water Development Board files).

Well J-17 (AY-68-37-203) in San Antonio is the most significant well in the San Antonio segment of the Edwards Aquifer since it is used as the index well for Bexar County, where more than 1.5 million people are supplied by water from the aquifer. Furthermore, regulations place restrictions on water use when the level in J-17 is less than 8.2 m above the level of Comal Springs. There is an excellent though non-linear correlation between the head in J-17 and Comal Springs discharge (Figure 13). The exponent of 0.66 in the regression equation indicates that flow is turbulent along a majority of the 40 km flow path between J-17 and Comal Springs.

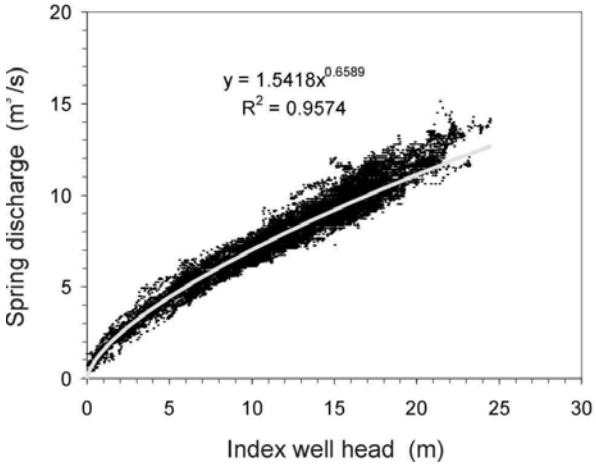

Figure 13 Correlation between the head in the Bexar County index well and the discharge from Comal Springs, based on daily readings between 1932 and 2002, showing a non-linear relationship indicative of turbulent flow in conduits (data from USGS and EAA data bases).

The velocities found from tracer tests in the San Antonio and Barton Springs segments of the Edwards Aquifer (Table 3) together with a larger global set of tracer test results (Worthington et al., 2000a) can be used with Comal Springs discharge data to estimate conduit size and flow regime by using the continuity equation

$$Q = v\,A \tag{2}$$

where Q is spring discharge, v is conduit velocity and A is conduit cross-section. Results are shown in Figure 14. It is unknown whether there is a single major conduit or a number of conduits in the main flow path to Comal Springs, but the figure indicates that flow is likely to be well within the turbulent flow regime.

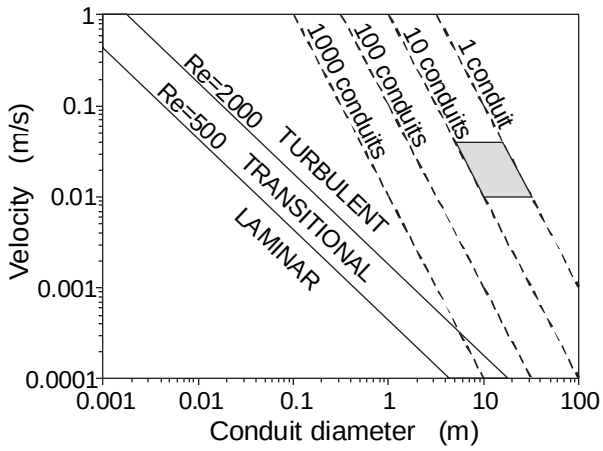

Figure 14 Conduit diameter, conduit velocity, and Reynolds Number for the conduit or conduits feeding Comal Springs. The most likely range of values is indicated by the shaded box.

Conclusions on the six tests

Each of the six tests provides evidence that flow in the Edwards Aquifer is more like an ideal karst aquifer than an ideal porous medium aquifer. This strongly supports the concept that there is an integrated network of conduits connecting the major sinking streams with the springs.

4 Locations of conduits based on aquifer structure

The Edwards Aquifer is notable not only for its large extent and high permeability but also for its extension to depths exceeding 1000 m below the water table. Karst theory can help in interpreting why this has occurred, and this interpretation will aid in identifying the location of conduits in the aquifer.

4.1 Theoretical optimum location of conduits

A first step in determining the locations of conduits in the Edwards Aquifer is to identify the optimum location for conduits. It has commonly been considered that shallow flow paths, close to the water table, are the most favored locations for conduits because the distance is shorter than for deeper flow paths and because fracture apertures are likely to be larger close to the land surface due to stress release (Thrailkill, 1968). However, Worthington (2001) showed that geothermal heating results in lower viscosity and greater flow at depth, and this can result in conduit formation deep below the water table in cases where sink to spring flow paths exceeds 3 km in length. Flow paths in the Edwards Aquifer greatly exceed 3 km, which indicates that conduit development deep below the water table is favored.

The three representative flow paths shown in Figure 15 were investigated to determine the most favorable location for conduit development in the aquifer. The input point for the flow paths is taken to be water sinking in the bed of Frio River and the output point is Comal Springs. Flow path A is the most direct pathway, is close to the water table, and assumes a linear decrease in head from 240 m at Frio River to 190 m at Comal Springs. The flow path is almost a straight line between the two end points and is 154 km long. Maclay (1995) suggests that large-displacement faults in northern Medina County are a barrier to flow. Flow path B follows a pathway that is parallel to most faults and thus minimizes the crossing of faults. Flow path C takes a southerly path deep in the confined zone of the aquifer and close to the Bad Water Line (the 1000 mg/L southerly limit of fresh water). Flow along the fractures in flow paths B and C is investigated at the middle of the Edwards Aquifer, which varies in thickness between 145m and 275 m along the flow paths analyzed.

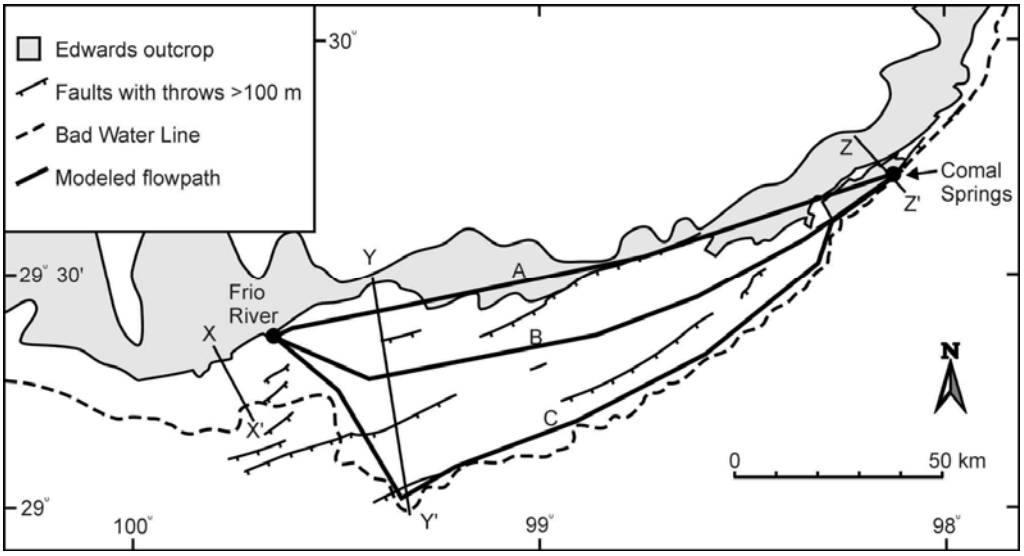

Figure 15 Three possible flow paths from sinks at Frio River to Comal Springs, showing a short path in the unconfined aquifer (A) and longer paths in the confined aquifer (B and C). The latter paths are favored for conduit development (see text for details).

The ambient groundwater temperature at 5 km increments along the three flow paths is shown in Figure 16a, assuming a surface temperature of 20.5 ^{0}C and a geothermal gradient of 0.0273 ^{0}C /m (Schultz, 1993). In northern Frio County the flow path descends to a depth of 1050 m below sea level, where the calculated ambient temperature is 55 ^{0}C. Discharge along the two flow paths is examined for a fracture width (w) of 1m and an aperture (b) of 0.1 mm. Flow along such a fracture is described by the Hagen-Poiseuille equation (which is also known as the cubic law)

$$Q = \Delta\, g\, b^3\, i\, w / 12\, : \qquad (3)$$

where Q is discharge, Δ is the density of water, g is gravitational acceleration, b is fracture aperture, i is hydraulic gradient and : is dynamic viscosity. Equation 3 can be simplified to

$$Q = g\, b^3\, i\, w / 12\, < \qquad (4)$$

where < is kinematic viscosity (:/Δ). Figure 16b shows the variation in kinematic viscosity along the three fracture pathways. Since g, b and w in equation 3 are constants in this analysis, this means that

$$Q \propto i / < \qquad (5)$$

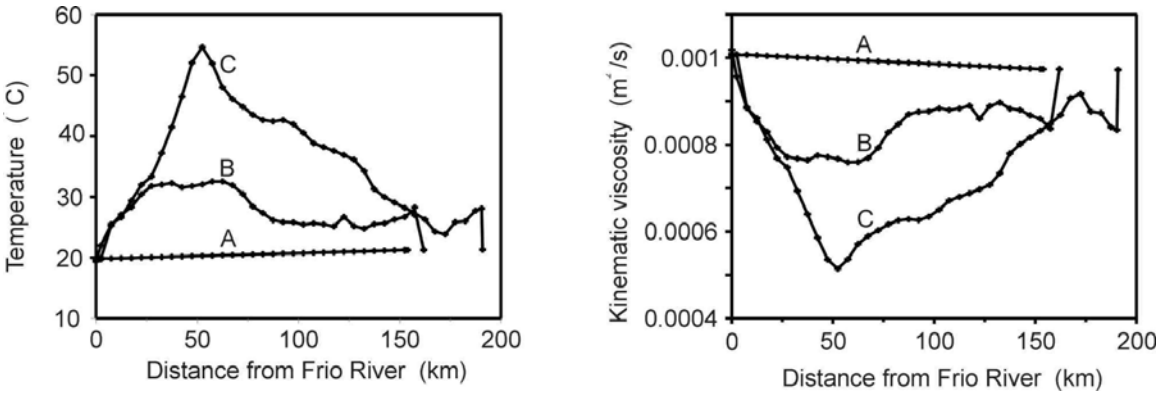

Figure 16 Temperature (left) and kinematic viscosity variations (right) along the three flow paths shown in Figure 15.

By assuming constant discharge along the length of each of these fracture pathways the hydraulic gradient can be calculated since it is inversely proportional to kinematic viscosity and the total head loss along the two pathways is 50 m. The final step is to calculate discharge along each of the two fracture pathways using Equation 4. Results are shown in Table 4.

Table 4 Characteristics of the three flow paths shown in Figures 15 and 16

Path	Length (km)	Relative length (%)	Discharge (L/s)	Relative discharge (%)
A	154	100	2.64E-10	100
B	162	105	2.94E-10	112
C	191	124	2.94E-10	112

The significance of the 12% greater flow along pathways B and C despite of the longer flow paths is that more dissolution takes place where there is greater flow. The development of conduits takes place by a positive feedback process, with the pathway having the greatest initial flow eventually developing into a conduit. The above comparison shows that deeper parts of the aquifer are favored over shallower parts for conduit development, even when the deep flow path is up to 24% longer than the shallow flow path.

4.2 Location of conduits based on structural, water level and water chemistry data

In the previous section it was shown that deep locations in the aquifer are favored over shallow locations for the development of conduits. Particularly favorable locations are in grabens and synclines since these offer the advantage of deeper flow paths without the disadvantage of the flow paths being longer. There are a number of large-scale structural troughs in the Edwards Aquifer, where there should be increased flow and where conduit development is favored (Figure 17). Three cross-sections of the aquifer (Figure 18) give further details of the structural troughs labeled X, Y, and Z in Figure 17.

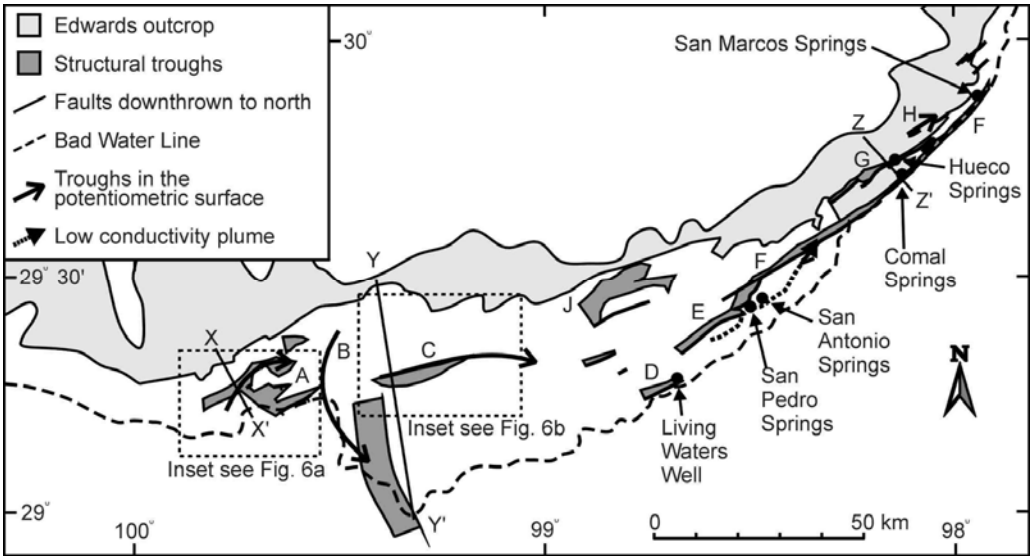

Figure 17 Indications of conduits in the Edwards Aquifer, based on structural troughs, potentiometric surface troughs, and a low conductivity plume of fresh water in Bexar County.

Nine major structural troughs are labeled A through J in Figure 17, and most of these have indications of conduits being associated with them. Feature A is a structural trough to the north of Big Mountain, where conduit development is favored just to the south of a fault (Figure 18, cross-section X). Water-level data show that a trough in the potentiometric surface is aligned with this structural trough (Figure 6). To the east there are three favored structural pathways and water-level data indicate that conduit development has taken place along pathway A in Figure 6a.

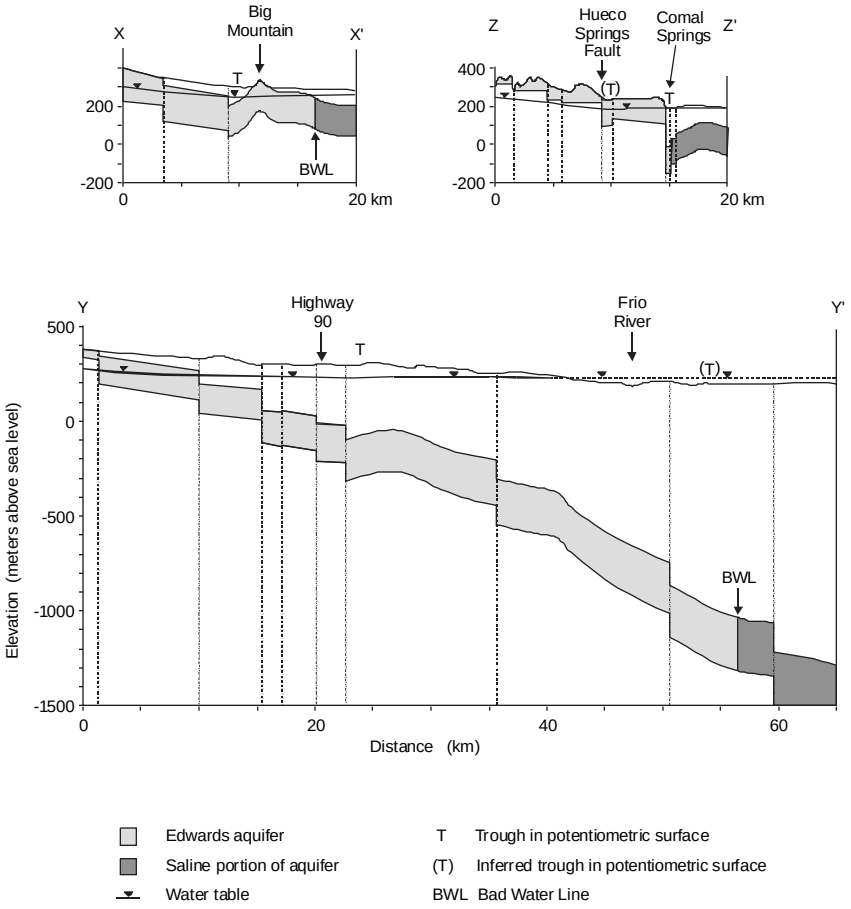

Figure 18 Aquifer cross-sections, showing the coincidence of structural troughs and potentiometric surface troughs. The locations of the cross-sections are shown in Figure 17 (structural data from Collins and Hovorka, 1997 and Guyton and Associates, 1979)

Feature B in Figure 17 is an enigmatic water-level trough. Flow in this trough is towards the south and water-level data in some wells at times of low flow are lower than measured levels to the east in Medina County. This area of the aquifer is complicated by the presence of igneous intrusives and by the scarcity of water-level data in southern Medina County, where the aquifer is deep below the surface and there are consequently few wells. There is increased sedimentation in the southern part of this pathway in a synclinal trough that plunges to the south, and conduit development in this trough may have facilitated the extension of the aquifer to the south.

Feature C in Figure 17 is a significant structural trough that coincides closely with a major potentiometric-surface trough (Figure 6b). The highly productive Living Waters Well is just north of a fault downthrown to the north (feature D). There is a deep graben (feature E) to the west of San Pedro and San Antonio Springs, which continued to the northeast to join feature F. The water-level data is insufficiently detailed in this area to indicate whether there is increased flow here, but the electrical conductivity data suggests that the main flow line is to the south of this graben. Feature F is an 80 km long feature that extends from near San Antonio Airport to San Marcos. Over much of its length it is a deep graben with an anticline to the south, and for the 50 km from Cibolo Creek to San Marcos the Bad Water Line is just south of the most favorable position for a conduit (Figure 18, cross-section Z). Comal Springs are on the northerly bounding fault of the graben and San Marcos Springs are about 100 m north of the graben (Hovorka et al., 1998). Feature G is a graben in Comal County with post-Edwards strata at the surface. Water-level data show this graben to be the northwesterly limit of the low-gradient potentiometric surface area, indicating high permeability along this graben. Furthermore, Hueco Springs is located on this graben. Feature H like feature G is a graben within the recharge zone where post-Edwards strata appear at the surface. George (1952) shows a potentiometric surface trough aligned with this graben. Finally, feature J is an extensive structural low but the structural trough rise steeply to the east so that is no favorable pathway for conduits to develop along, and the major flow in the confined aquifer is 10-30 km south of J.

The close alignment between potentiometric surface troughs and at least parts of six of the nine structural troughs and the position of the highest-production well in the Edwards Aquifer in the seventh trough strongly support the hypothesis that favorable structural location is an important factor in conduit development in the aquifer.

In Bexar County it is not possible to identify potentiometric-surface troughs because of the large abstraction rates for use by the city of San Antonio together with the low hydraulic gradients in the confined aquifer. However, the high density of wells in this area with water-quality data permits the identification of a low electrical conductivity (EC) plume of fresh water in the southern part of the confined aquifer. This is shown on an aquifer-scale map by Hovorka et al. (1996, Figure 6), and is shown in more detail in Figure 19. Some EC values in southwest San Antonio are less than 440 :S/cm, suggesting rapid flow from the recharge zone of this dilute water. To the east there appears to be a steady increase of the dilute water plume to 480 :S/cm in

northeast San Antonio and to 520 :S/cm at Comal Springs. The plume lies just to the south of the Bexar County index well (J-17) and San Pedro and San Antonio Springs.

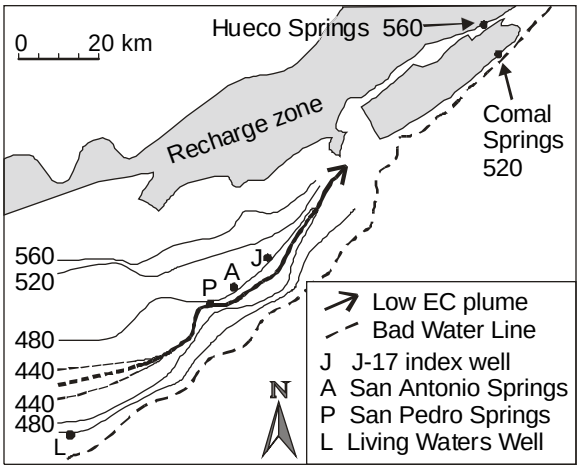

Figure 19 Plume of low electrical conductivity (EC) in southern Bexar County, with EC values in µS/cm (based on data from Texas Water Development Board files).

4.3 Development of the aquifer over time

The conditions that favor enhanced dissolution in structural troughs can help explain not only current conduit locations but also the development of the aquifer over time. Pertinent questions include:

(1) Why does the confined aquifer vary in width from less than 1 km at Comal Springs (section Z in Figures 17 and 18) to more than 50 km in Medina County (section Y in Figures 17 and 18), and how have discharge points from the aquifer varied over time?

(2) Can aquifer development in the past be understood in terms of current processes, and if so what is the current rate of aquifer development?

(3) Where is most aquifer dissolution taking place, and is the Bad Water Line stable or is it moving to the south?

Variation in the width of the confined aquifer

The uplift and faulting along the Balcones Fault Zone in early Miocene times can be considered as the beginning of the modern phase of aquifer development (Sharp and Banner, 1997). At the present time, recharge occurs where the aquifer is unconfined and natural discharge occurs from springs. All the major springs in the aquifer discharge from faults that have substantial displacements, with the flow rising up the faults through up to 200 m of strata that overlie the Edwards Aquifer. It is likely that similar patterns of recharge and discharge have taken place since the Balcones Fault Zone was established in the Miocene.

The large variation in width of the confined zone is a marked characteristic of the aquifer. The reasons for this can best be illustrated by examining cross-sections where the confined zone is at its narrowest and at its widest. These are shown in cross-sections Z-Z' and Y-Y', respectively, in Figures 17 and 18.

Cross-section Z-Z' is at Comal Springs, where the fresh-water zone is limited to a narrow graben. The top of the Edwards aquifer is just below sea level, but to the south there is an anticline where the strata rise more than 100 m. The deep graben provides a much more favorable location for aquifer dissolution and thus enhanced flow than the anticline to the south (Worthington, 2001 and section 4 above). This has effectively provided a barrier to the southward migration of the Bad Water Line, which is less than 500 m from Comal Springs. The graben and associated anticlinal barrier to southward migration of the Bad Water Line is present throughout Comal County and extends west in Bexar County and east into Hays County. This is a major reason why the confined zone in the eastern part of the aquifer is so narrow.

The central part of the Edwards aquifer is much wider, reaching a maximum width of 54 km in western Medina County. The cross-section at that point shows southward-dipping strata except for just south of Highway 90, where there is a structural trough to the north of an anticline (Figure 18, section Y-Y'). There is a potentiometric surface trough that is coincident with the structural trough, and this demonstrates that there is increased flow along the trough (Figure 6). The structural trough extends for about 25 km. In this area the trough provides a focus for enhanced dissolution and flow and the anticline immediately to the south provided a structural barrier to southward migration of the Bad Water Line. However, to the west this anticline dies out and so there was no impediment to continuous migration of the Bad Water Line to the south (flow path B in Figure 17). However, the presence of this marked trough in the potentiometric

surface (Figure 6 and C in Figure 17) does suggest that it may have been the major vector for eastward flow in this part of the aquifer for some considerable period. At such a time it is quite possible that the Bad Water Line was just to the south of the trough in an analogous situation to that at Comal Springs today.

It was noted above in Section 4.2 that enhanced flow usually but not always occurs along structural troughs. From the discussion above considering the preferential flow at the cross-sections X, Y, and Z, it does appear that the major differences in the width of the confined zone of the aquifer is explained by the locations of structural troughs and the enhanced dissolution that occurs in them (Worthington, 2001).

The confined zone in the western part of the aquifer is much narrower than in the central part. In central Uvalde County there is a structural dome in the Edwards strata, with several inliers of Edwards Group strata, such as at Big Mountain, which is just east of the city of Uvalde (cross-section Z-Z' in Figures 17 and 18). To the north of Big Mountain there is a structural trough, and this forms a favorable location of enhanced dissolution and flow. This is confirmed by the presence of a trough in the potentiometric surface that closely follows the structural trough (Figure 6).

Dissolution rates and rate of aquifer evolution

There are a number of dissolution processes taking place in the aquifer, and these all serve to enhance aquifer porosity and permeability. An estimate of current aquifer dissolution rates is given in Table 5. This is based on the difference between dissolved solids in aquifer recharge and aquifer discharge. Aquifer recharge is calculated from mean concentrations of the six major ions from three rivers that recharge the aquifer. Aquifer discharge is taken as the average of San Antonio Water System, Comal Springs, and San Marcos Springs averages. These averages are not weighted by discharge, and clearly could be refined using more locations, more measurements at each location, and by weighting the data by discharge. However, for all six ions both the recharge and discharge data are clustered and distinctly different, and so give a reasonable approximation.

Table 5 Average major ion concentrations in aquifer recharge and discharge

	n	Ca^{++}	Mg^{++}	Na^{+}	HCO_3^{-}	SO_4^{--}	Cl^{-}
Frio River (1)	30	54.1	11.4	6.0	202	13.3	10.2
Nueces River (1)	30	61.8	9.9	5.3	207	11.0	10.3
Blanco River (1)	30	67.1	12.2	6.0	243	15.0	10.3
Recharge average		**60.6**	**11.2**	**5.8**	**218**	**13.1**	**10.3**
SAWS	(2)	80.0	14.0	10.7	267	25.8	20.5
Comal Spring (3)	32	78.4	16.1	9.4	285	24.1	16.6
San Marcos Spring (3)	19	83.7	17.8	10.2	312	23.9	20.1
Discharge average		**80.7**	**16.0**	**10.1**	**288**	**24.6**	**19.1**
Aquifer dissolution		**20.1**	**4.8**	**4.3**	**69.6**	**11.5**	**8.8**

Notes: (1) USGS (2003); (2) Averages from 1997-2002 data; (3) from EAA Hydrogeologic reports for 2001 and 2002 and from TWDB online database

Aquifer dissolution is calculated from the difference between the recharge and discharge concentrations (Table 5). This is then converted into an equivalent concentration of minerals removed, assuming that the six ions are derived from dolomite, anhydrite, calcite and halite. The overall ion balance error in this calculation was 0.7%. The mean discharge from the aquifer over the period of record (1934-2002) is 8.34×10^8 m^3/year or 676,500 acre-feet per year (EAA, 2003). The flux of minerals removed is calculated from the product of aquifer dissolution and aquifer discharge, and converted to a volume of 25,700 m^3 of rock that is removed each year as dissolved load (Table 6).

Table 6 Flux of minerals removed from the aquifer as solutes

	Dolomite	Anhydrite	Calcite	Halite	Total
Aquifer dissolution (mg/L)	36.6	16.3	18.4	13.1	84.4
Flux of minerals removed (t/year)	30500	13600	15300	10900	70300
Specific gravity	2.85	2.93	2.71	2.30	2.73
Flux of minerals removed (m^3/year)	10700	4640	5650	4730	25700

Total aquifer porosity has been estimated to be 2.13 x 10^{11} m3 (Hovorka et al., 1996), and dividing this by the annual flux of 25,700 m^3 of minerals gives an estimate of 8.3 million years for the age of the aquifer. However, this calculation makes the assumption that aquifer porosity at the beginning of the Miocene was zero and that dissolution since the uplift of the Balcones Fault Zone has created the modern average porosity of 18%. This is unrealistic since there is substantial porosity in the saline zone south of the Bad Water Line (Hovorka et al., 1996), and thus the initial porosity in the Edwards before the Miocene must also have been substantial. Deike (1990) measured the porosity of cores on either side of the Bad Water Line and found that the core in the fresh-water zone had a porosity of 44%, compared to 20% for core in the saline zone. An increase in calcite and an almost total removal of dolomite indicated that dedolomitization close to the Bad Water Line was the major dissolution process (Deike, 1990). If half of the modern porosity of 18% has been created by modern (i.e. post early-Miocene) dissolution processes then the calculated age of the aquifer is 16.6 million years, which is within the early Miocene (16- 24 million years before present). These calculations show that the development of the Edwards Aquifer since the early Miocene can be explained in terms of modern dissolution rates.

Location of aquifer dissolution and movement of the Bad Water Line

There are a number of dissolution processes taking place in the aquifer at present. These include:

i) dissolution of calcite and dolomite by water undersaturated with respect to these two minerals. Creeks recharging the aquifer drain from the limestones of the Edwards Plateau aquifer and have high dissolved solids concentrations in most conditions, but much lower dissolved solids following major rain events. Much of the calcite dissolution and some of the dolomite dissolution will take place in the unsaturated zone and will result in lowering of the bedrock surface.

ii) dissolution of gypsum. Springs and wells in the Edwards Aquifer typically have concentrations <5% of saturation, showing that there is little gypsum or anhydrite present. However wells south of the Bad Water Line have far higher concentrations. Schultz and Halty (1997) found that anhydrite beds are almost absent to the north of the Bad Water Line and thicken significantly to the south of it (Figure 20). This suggests that dissolution of anhydrite

close to the Bad Water Line has been associated with southward movement of that line and associated enlargement of the fresh-water zone of the Edwards Aquifer.

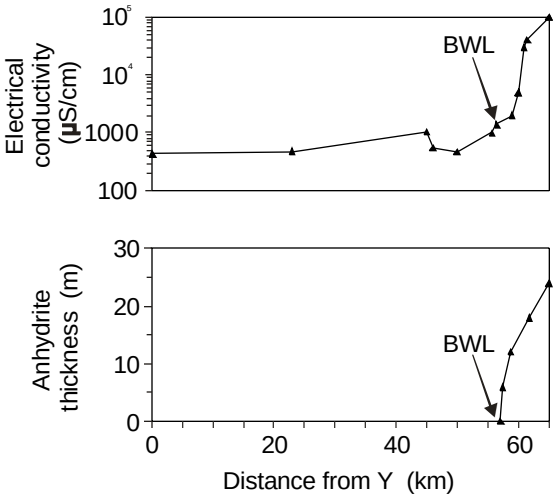

Figure 20 Correlation between the position of the Bad Water Line and the thickness of anhydrite in Edwards Group strata along the section Y-Y' in Figures 17 and 18 (based on data from Schultz and Halty, 1997)

iii) mixing corrosion at the Bad Water Line of solutions with differing hydrogen sulfide concentrations. The Edwards aquifer has high oxygen and low H_2S concentrations, whereas the saline zone has low oxygen and high H_2S concentrations, with oil-field brines thought to be the source of the H_2S (Rye et al., 1981). The mixing of these contrasting waters at the Bad Water Line can result in substantial dissolution of calcite or dolomite (Palmer, 1991).

iv) mixing corrosion at the Bad Water Line of solutions with differing CO_2 concentrations. As with H_2S, the mixing of waters with differing CO2 concentrations can result in substantial dissolution of calcite or dolomite (Palmer, 1991).

v) dedolomitization. Dedolomitization at the Bad Water Line in the Edwards aquifer has been documented by Abbott (1975) and Deike (1990).

The first of the five processes above is likely to occur predominantly in the unsaturated zone, but the remaining four occur predominantly close to the Bad Water Line, where possibly half of the total dissolution takes place. The migration rate (m) to the south of the Bad Water Line can be calculated as a first approximation from equation 6.

$$m = f\, n / (L\, z) \qquad (6)$$

where f is the flux of dissolved minerals removed from the area of the Bad Water Line, n is the increase in porosity at the Bad Water Line, L is the length of the Bad Water Line (about 300 km between the western and eastern divides, at Brackettville and Kyle, respectively), and z is aquifer thickness (190 m). The average migration south of the Bad Water Line is 2.5 mm per year, assuming a porosity increase of 9% at the Bad Water Line. This movement is equivalent to a total migration of 40 km over 16 million years. This is more than the 30 km average width of the aquifer at present. However, surface erosion over the last 16 million years must have removed a substantial thickness of the aquifer, and the 40 km estimate is of the correct magnitude.

The above calculations demonstrate that current aquifer dissolution processes can be used to explain the development of the aquifer since the early Miocene, and that the current migration rate to the south of the Bad Water Line is roughly 2.5 mm per year. This model is very different from earlier models.

Abbott (1975) suggested that the fresh-water circulation in the aquifer commenced during the Miocene, but thought that the Bad Water Line represents "an early bypass boundary of the aquifer that has become deeply engrained with time" (Abbott, 1975, p. 251). It is difficult to see how fresh-water flow could have been quickly established in the early evolution of the aquifer along a circuitous flow path to depths exceeding 1000 m below sea in southern Medina County.

Deike (1990) suggested that a major part of the aquifer could have formed in the last 10,000 years. This rate is more than three orders of magnitude more rapid than the rate calculated above. This would have resulted in solute concentrations of calcium, magnesium, sulfate and bicarbonate that are far in excess of solubility limits, and so such a short period of development is not likely.

The present model postulates the progressive and gradual migration southward of the Bad Water Line since aquifer initiation in the Miocene. The evidence from current dissolution rates and solute fluxes supports the model, with much of the current dissolution taking place at the Bad Water Line, which is migrating south at an average rate of about 2.5 mm/year.

4.4 Recommended location of conduits for the USGS MODFLOW model

The major principles guiding the location of conduits for the MODFLOW model are as follows:

1) As far as possible the distribution of permeability should result in honoring the most comprehensive potentiometric surface maps of the aquifer. The most detailed potentiometric surface maps of the aquifer are in a series of county-scale USGS Water-Supply Papers (Livingston et al., 1936; Sayre, 1936; George, 1952; Holt, 1959; Arnow, 1963; DeCook, 1963; Welder and Reeves, 1964), supplemented by a detailed survey of the San Marcos area by Ogden et al. (1986). Together these reports have 345 water-level measurements.

2) Both theoretical investigations (numerical models of dissolution of carbonate aquifers) and empirical evidence (more than 10,000 tracer tests) provide unequivocal evidence that continuous conduits connect sinking streams and springs in carbonate aquifers. Thus the major sinking rivers should be connected to the major springs by conduits. This can be accomplished by introducing continuous lines of high-K cells that connect the sinking streams with the main springs. This makes the Aconduits@ a quarter mile wide. This is some 20-50 times wider than the actual likely width of the major conduits in the Edwards Aquifer. This is the closest approximation that can be made with the current model.

3) The major potentiometric surface troughs in the aquifer (near Uvalde, D=Hanis and in Comal County) coincide with structural grabens, and carbonate dissolution theory indicates that grabens are a favorable location for conduit development. Thus grabens are used as a guide for locating conduits.

4) In Bexar County there is a plume of water with EC similar to or lower than at Comal Springs, and this provides an excellent indicator of preferential flow, suggesting a major conduit (or conduits). This putative conduit passes about 2 km southeast of J-17. By contrast, the area northwest of J-17 extending up to the recharge zone generally has a much higher EC than Comal Springs and so cannot be on the highest permeability pathway to the springs.

5) Dissolution and the preferential development of conduits is favored on theoretical grounds in the deeper parts of the aquifer. Expansion of the aquifer to the south seems to have been inhibited in Uvalde County by volcanic aquitards and in Comal and Hays counties by a major anticline immediately to the southeast of the Bad Water Line. In Bexar County the water-

quality data suggest the highest *K* is in a zone less than 2 km wide and is 3 - 5 km from the Bad Water Line. The same may well occur in Medina County and in western Uvalde and eastern Kinney counties, but there is very little head or chemistry data close to the Bad Water Line to test this hypothesis.

6) The southeast trend of the Bad Water Line south of Knippa may be associated with a thickening of the Edwards sequence and a syncline at the base of the Edwards. The Edwards Group is over 900 feet thick close to the Bad Water Line in Frio County. The syncline is several kilometers east of the Bad Water Line, and it seems quite likely that conduit development in this area has preferentially occurred in this syncline.

The location of conduits in Figure 21 is based on the above principles. The numbers below are keyed to the numbers on the figure.

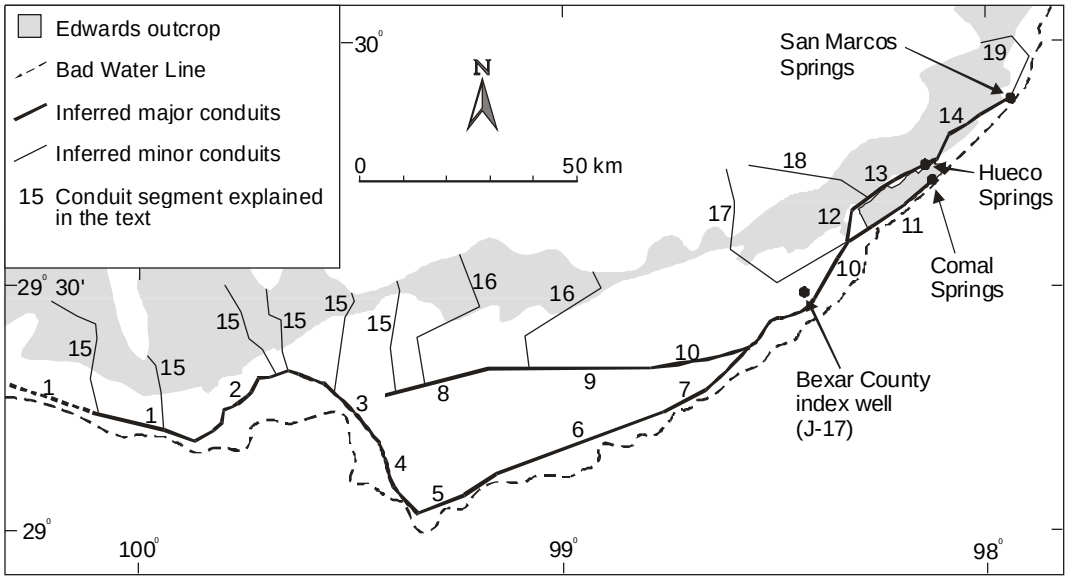

Figure 21 Location of conduit networks connecting the major sinking streams and the major springs.

1) A conduit parallel to and some 1-3 miles from the Bad Water Line. This could be extended to the west towards the divide if this helps the MODFLOW simulation. The head data close to the Brackettville divide are sparse and a conduit in Kinney County is less important than further east since there is only a small flux of water moving eastward in this area.

2) There is strong evidence for this conduit crossing the Uvalde structural dome. It is the northernmost of three possible pathways shown in Figure 6.

3) Head data shows that flow to the south of Knippa is to the southeast.

4) The conduit shown follows the axis of the syncline.

5) Once the synclinal axis crosses the major fault that is downthrown to the south then the favored pathway is to the east on the downthrown side of the fault.

6) There is sparse data in this area, but other evidence suggests the conduit is 1-3 miles north of the Bad Water Line.

7) There is a fault here that is downthrown to the north, which favors development of a conduit parallel to and just north of the fault. From the eastern termination of the fault the conduit seems to trend away from the Bad Water Line and is intersected by the Living Waters (catfish farm) well. It then joins the other major conduit (see 10, below).

8) Potentiometric surface maps define a deep trough here, suggesting the conduit is just south of a fault that extends from just into Uvalde County almost as far as Hondo. Close to Hondo a fault to the south makes the structure a graben. The conduit is situated in the graben (Figure 6). It is likely that this conduit was developed before the aquifer extended into south Medina County, and at that time would have carried the flow from Uvalde County. It is possible that this flow path still carries much of the flow from Uvalde County.

9) The exact position of the conduit is poorly defined in this area. It seems to pass south of Castroville. Possibly the line of the conduit should be curved (concave to the north) rather than the straight line shown in Figure 9.

10) The conduit is well defined in Bexar County by the water chemistry data (Figure 19).

11) The conduit is close to and on the downthrown (south) side of the Comal Springs fault. It is shown as ending at Comal Springs but it is possible that it continues close to the Bad Water Line as far as San Marcos Springs.

12) Head and water-quality data suggest that some of the discharge from Bexar County flows to the NNE through this structurally low area with complex minor faulting.

13) The conduit is along the graben where post-Edwards strata outcrop at the surface. Hueco Springs are on the conduit.

14) Head data suggest the conduit at this point heads NNE to flow NE on the northern, downthrown, side of two faults. There are outcrops of post-Edwards strata in places on the northern side of these faults. In the final few miles there is an absence of strong evidence of where the conduit is located, so it is shown as a straight line to San Marcos Springs.

15) Flow in the Edwards Aquifer is in the same direction as the flow of most major sinking or losing rivers (West Nueces, Nueces, Dry Frio, Frio, Sabinal, Seco, Hondo, and Medina). Major conduits are likely to be parallel to and quite close to these rivers except they are unlikely to follow all the meanders of the surface rivers. These are shown in a very simplified fashion in Figure 20. The conduits continue downdip (roughly southerly) direction in the confined aquifer for each of these sinking rivers to join up with the major strike-oriented conduits.

16) The 1951 and 1952 potentiometric surface maps (Holt, 1959) indicate flow to the south in the confined aquifer is blocked by faults. The head data suggest the conduit from Hondo Creek flows south-west and then south to join the major conduit (#8) to the west of D'Hanis. The Medina conduit appears to flow to the southwest on the northern side of Haby Crossing Fault where the displacement is 600 - 900 ft. West of Quihi the displacement rapidly diminishes, and the head data suggest that the conduit heads south here.

17) Cibolo Creek generally flows parallel to the potentiometric surface in the Glen Rose formation. Mace et al. (2000) give a detailed potentiometric surface map that shows that all the flow upstream of Camp Bullis is directed to a deep trough in the potentiometric surface, which enters the Edwards Aquifer close to UTSA. However, other water-level data challenge the existence of this trough (A. Schultz, 2003, personal communication). Water level and electrical conductivity data suggest flow in the confined aquifer is to the southeast as far as the graben north of the Alamo Heights Horst (Groschen, 1996). The conduit is then likely to follow the graben towards Comal Springs.

18) Head data suggest that groundwater flow under Cibolo Creek east of Camp Bullis is parallel to Cibolo Creek as far as the sharp bend where the creek turns south. Flow from there is likely to be to the southeast. The easterly flow parallel to Cibolo Creek is confirmed by mapping in Honey Creek Cave, where an east-flowing stream has been found in the southern part of the cave (Veni, 1994).

19) Blanco River flows parallel to the general potentiometric surface as it crosses the Edwards outcrop. The conduit probably roughly underlies the river and then curves to the east towards the Bad Water Line and then south. It may well parallel the Bad Water Line as it approaches San Marcos Springs. The head data in this area are sparse, and some data suggest flow from the Blanco River is towards Barton Springs.

It should be noted that the conduit locations described above and shown in Figure 20 are based on an analysis of the data described earlier, and are considered to be suitable for the current USGS MODFLOW simulation. Some refinement of the conduit network has taken place in 2002/2003 during the calibration by the USGS of the MODFLOW model. Furthermore, recent work by Hovorka et al. (2003) has examined some aquifer data in more detail and is producing an independent assessment of conduit locations.

The new USGS MODFLOW model represents a significant improvement over previously available numerical models of the Edwards aquifer. Among new features, it incorporates a greatly refined cell size, much better estimates of pumping stresses, and a representation of the high-permeability zones or conduits. The model is calibrated to the whole lateral extent of the aquifer rather than just one well (J-17) and two springs, which was the primary purpose of the previous model (GWSIM). Furthermore, the model can be use with a modern, user-friendly interface, and thus has the potential of being much more widely used than earlier models.

It is inevitable that there are a number of possible improvements that could be made to the model in the future. The model is designed for aquifer-scale rather than local-scale simulations, and is limited to some extent by having a quarter-mile cell width, a single layer, by using a monthly time step, and by assuming homogeneity of properties within each cell. A similar model has been prepared for the neighboring Barton Springs segment of the Edwards Aquifer, and Scanlon et al. (2003) discuss the uses and limitations of such models. Refinement of properties such as

the time step used and the incorporation of turbulent flow in future models could potentially facilitate a better simulation of flow and transport in the aquifer, though more field data would be required. Turbulent flow in conduits has been simulated in research models (Clemens et al., 1996; Liedl et al., 2003), but such models are not yet commercially available.

References

Abbott, P.L., 1975, Calcitization of Edwards Group dolomites in the Balcones fault zone aquifer, south central Texas: Geology, v. 2, no. 7, p. 359-62.

Arnow, T., 1963, Ground-water geology of Bexar County, Texas: U.S. Geological Survey Water-Supply Paper 1588, 36 p. [Also published as Texas Board of Water Engineers Bulletin 5911, 62 p., 1959].

Atkinson, T.C., and P.L. Smart, 1981, Artificial tracers in hydrogeology. In: A survey of British hydrogeology 1980. Royal Society, London, 173-190.

Berner, R.A., and J.W. Morse, 1974, Dissolution kinetics of calcium carbonate in sea water, IV, Theory of calcite dissolution, American J. Science, 274, 108-134.

Clemens, T., Hückinghaus, D., Sauter, M., Liedl, R., and Teutsch, G., 1996, A combined continuum and discrete network reactive transport model for the simulation of karst development. In: Model Calibration and Reliability (Eds. K. Kovar and P. van der Heijde), IAHS Publ. No. 237, 309-318.

Collins, E.W., and Hovorka, S.D., 1997, Structure map of the San Antonio Segment of the Edwards Aquifer and Balcones Fault Zone, south central Texas: Structural framework of a major limestone aquifer: Kinney, Uvalde, Medina, Bexar, Comal, and Hays counties, Bureau of Economic Geology, University of Texas at Austin, Miscellaneous. Map No. 38, 14 p.

DeCook, K.J., 1963, Geology and ground-water resources of Hays County, Texas: U.S. Geological Survey Water-Supply Paper 1612, 72 p.

Deike, R.G., 1990, Dolomite dissolution rates and possible Holocene dedolomitization of water-bearing units in the Edwards Aquifer, south central Texas: Journal of Hydrology, v. 112, no. 3/4, p. 335-373.

Dole, R.B., 1906, Use of fluorescein in the study of underground waters, in Fuller, M.L., Underground-water papers, 1906. U.S. Geological Survey Water-Supply Paper 160, p. 73-85.

Dreybrodt, W., 1996, Principles of early development of karst conduits under natural and man-made conditions revealed by mathematical analysis of numerical models, Water Resources Research, 32, 2923-2935.

EAA (Edwards Aquifer Authority), 2003, Edwards Aquifer Hydrogeologic report for 2002, Report. Available online at edwardsaquifer.org.

Freeze, R.A. and J.A. Cherry, 1979. Groundwater. Prentice-Hall, Englewood Cliffs, NJ, 604p

George, W.O., 1952, Geology and ground-water resources of Comal County, Texas: U.S. Geological Survey Water-Supply Paper 1138, 126 p.

Groschen, George E., 1996, Hydrogeologic factors that affect the flowpath of water in selected zones of the Edwards Aquifer, San Antonio region, Texas: U.S. Geological Survey, Water Resources Investigations Report 96-4046, 73 p.

William F. Guyton and Associates, 1979, Geohydrology of Comal, San Marcos, and Hueco Springs: Texas Department of Water Resources Report 234, 85 p.

Halihan, T., J.M. Sharp, Jr., and R.E. Mace, 1999, Interpreting flow using permeability at multiple scales, In: Karst modeling, Eds. A.N. Palmer, M.V. Palmer and I.D. Sasowsky, Special Publication No. 5, Karst Waters Institute, Charles Town, WV, 82-96.

Halihan, T., R.E. Mace and J.M. Sharp, Jr., 2000, Flow in the San Antonio segment of the Edwards Aquifer: matrix, fractures, or conduits? In: Groundwater flow and contaminant transport in carbonate aquifers, Eds. C.M. Wicks and I.D. Sasowsky, Balkema, Rotterdam, p. 129-146.

Hauwert, N.M., Sansom., J.W.Jr., Johns, D.A, and Aley, T.A., 2002a, Groundwater tracing study of the Barton Springs segment of the Edwards Aquifer, southern Travis and northern Hays Counties, Texas, Barton Springs/ Edwards Aquifer Conservation District and City of Austin Watershed protection Department.

Hauwert, N.M., Johns, D.A, Sansom., J.W., and Aley, T.J., 2002, Groundwater tracing of the Barton Springs Edwards Aquifer, Travis and Hays counties, Texas, Gulf Coast Association of Geological Societies Transactions, 52, 377-384.

Hauwert, N.M., D.A. Johns, and J. Sharp, 2002b, Evidence of discrete flow in the Barston Springs segment of the Edwards Aquifer. In: Hydrogeology and biology of post-Paleozoic carbonate aquifers (eds. J.B. Martin, C.M. Wicks and I.D. Sasowsky). Karst Waters Institute, Charles Town, WV, Special Publication No. 7, p. 62-167.

Hess, J.W., and W.B. White, 1988, Storm response of the karstic carbonate aquifer of southcentral Kentucky, Journal of Hydrology, 99, 235-252.

Holt, C.L.R., Jr., 1959, Geology and ground-water resources of Medina County, Texas: U.S. Geological Survey Water-Supply Paper 1422, 213 p. [Also published as Texas Board of Water Engineers Bulletin 5601, 278 p., 1956].

Hovorka, S.D., A.R. Dutton, S.C. Ruppel and J.S. Yeh, 1996, Edwards Aquifer ground-water resources: geologic controls on porosity development in platform carbonates, South Texas, Report of Investigations No. 238, Bureau of Economic Geology, Austin, 75p.

Hovorka, S.D., Mace, R.E., and Collins, E.W., 1998, Permeability structure of the Edwards Aquifer, South Texas - Implications for Aquifer Management, Bureau of Economic Geology, University of Texas at Austin, Report of Investigation No. 250, 55 p.

Hovorka, S.D., Phu, T,, Nicot, J.P., and Lindley, A., 2003, Refining the conceptual model for flow in the Edwards Aquifer - characterizing the role of fractures and conduits in the Balcones fault zone segment. Report in preparation for the Edwards Aquifer Authority.

Huntoon, P. W., 1995, Is it appropriate to apply porous media groundwater circulation models to karstic aquifers?, in Groundwater models for resources analysis and management, Ed. A. I. El-Kadi, Lewis Publishers, Boca Raton, 339-358.

Klemt, W.B., Knowles, T.R., Elder, G.R., and Sieh, T.W., 1979, Ground-water resources and model applications for the Edwards (Balcones fault zone) aquifer in the San Antonio region, Texas: Texas Department of Water Resources Report 239, 94 p.

Liedl, R., Sauter, M., Hückinghaus, D., Clemens, T., and Teutsch, G., 2003, Simulation of the development of karst aquifers using a coupled continuum pipe flow model, Water Resources Research, 39.

Livingston, P.P., Sayre, A.N., and White, W.N., 1936, Water resources of the Edwards Limestone in the San Antonio area, Texas: U.S. Geological Survey Water-Supply Paper 0773-B, p. 59-113.

Mace, R.E., Chowdhury, A.H., Anaya, R., Way, S-C, 2000, Groundwater availability of the Trinity Aquifer, Hill Country area, Texas: numerical simulations through 2050, Texas Water Development Board, Report 353, 169 p.

Maclay, R.W., 1995, Geology and hydrology of the Edwards Aquifer in the San Antonio area, Texas, U.S. Geological Survey Water-Resources Investigations Report 95-4186, 64p.

Maclay, R.W, T.A. Small, and P.L. Rettman, 1981, Application and analysis of borehole data for the Edwards Aquifer in the San Antonio area, Texas. Texas Department of Water Resources, Limited Publication No. 131, 88 p.

Maclay, R.W., and Land, L.F., 1988, Simulation of flow in the Edwards Aquifer, San Antonio region, Texas, and refinement of storage and flow concepts: U.S. Geological Survey Water-Supply Paper 2336-A, 48 p.

Ogden, A.E., R.A. Quick, S.R. Rothermel and D.L. Lunsford, 1986, Hydrogeological and hydrochemical investigations of the Edwards Aquifer in the San Marcos area, Hays County, Texas. Edwards Aquifer Research and Data Center, San Marcos, Texas, 364 p.

Palmer, A.N., 1981, A geological guide to Mammoth Cave National Park. Zephyrus Press, Teaneck, New Jersey, 196p.

Palmer, A.N., 1991. Origin and morphology of limestone caves. Geol. Soc. Amer. Bull., 103, 1-21.

Plummer, L.N., and T.M.L. Wigley, 1976, The dissolution of calcite in CO_2-saturated solutions at 25^{o}C and 1 atmosphere total pressure. Geochim. Cosmochim. Acta, 40, 191-202.

Quinlan, J.F., Ewers, R.O., and Palmer, A.N., 1986, Hydrogeology of Turnhole Spring groundwater basin, Kentucky, *in* Geological Society of America Centennial Field Guide - Southeastern Section, p. 7-12.

Rothermel, S.R., Ogden, A.E., and Snider, C.C., 1987, Hydrochemical investigation of the Comal and Hueco Spring systems, Comal County, Texas: San Marcos, Texas, Southwest Texas State University, Edwards Aquifer Research and Data Center Report R1-87, 182 p.

Rye, R.O., Back, W., Hanshaw, B.B., Rightmire, C.T., and Pearson, F.J., Jr., 1981, Origin and isotopic composition of dissolved sulfide in groundwater from carbonate aquifers in Florida and Texas: Geochimica et Cosmochimica Acta, v. 45, no. 10, p. 1,941-1,950.

Sayre, A.N., 1936, Geology and ground-water resources of Uvalde and Medina Counties, Texas: U.S. Geological Survey Water-Supply Paper 678, 146 p.

Scanlon, B.R., Mace, R.E., Barrett, M.E., and Smith, B., 2003, Can we simulate flow in a karst system using equivalent porous media models? Case study, Barton Springs Edwards Aquifer, USA, Journal of Hydrology, 276, 137-158.

Schindel, G.M., 2002, General Manager's Report

Schindel, G.M., Johnson, S., Worthington, S.R.H., Alexander, E.C., Jr., Alexander, S., and Schnitz, L., 2002, Groundwater flow velocities for the deep artesian portion of the Edwards Aquifer, near Comal Springs, Texas, Geological Society of America Annual Meeting Abstracts.

Schultz, A.L., 1993, Defining the Edwards Aquifer freshwater/saline-water interface with geophysical logs and measured data-San Antonio to Kyle, Texas: San Antonio, Texas, Edwards Underground Water District Report 93-06, 81 p.

Schultz, A.L., and Halty, S.R., 1997, Anhydrite: source of high sulfate concentrayion near Edwards Aquifer "Bad-Water" Line, Bulletin of the South Texas Geological Society, 37(9), 11-16.

Sharp, J.M., and Banner, J.L., 1997, The Edwards Aquifer: a resource in conflict. GSA Today, 7(8), 1-9.

Street, R.L., Watters, G.Z., and Vennard, J.K., 1996, Elementary fluid mechanics, Wiley, New York, 757 p.

Swanson, G.J., 1991, Super well is deep in the heart of Texas: Water Well Journal, v. 45, no. 7, p. 56-58.

Thorkildsen, D.F., and McElhaney, P.D., 1992, Model refinement and applications for the Edwards (Balcones Fault Zone) Aquifer in the San Antonio Region, Texas, Texas Water Development Board Report 340.

Thrailkill, J., 1968, Chemical and hydrologic factors in the excavation of limestone caves. Geological Society of America Bulletin 79, 19-46.

Tomasko, D., Fisher, A.-M., Williams, G.P., and Pentecost, E.D., 2001, A statistical study of the hydrological character of the Edwards Aquifer. Argonne National Laboratory, Chicago, 38 p. plus figures and appendices.

USGS, 2003, Online database of water quality data

Veni, G. E., 1994, Geomorphology, hydrogeology, geochemistry, and evolution of the karstic lower Glen Rose Aquifer, south-central Texas, Pennsylvania State University at University Park, University Park, PA, USA, Ph.D. dissertation, 749 p.

Welder, F.A., and Reeves, R.D., 1964, Geology and ground-water resources of Uvalde County, Texas: U.S. Geological Survey Water-Supply Paper 1584, 49 p.

White, W.B. and White, E.L., 1989, Karst hydrology: concepts from the Mammoth Cave area, (Eds.), Van Nostrand Reinhold, New York, 346 p.

Worthington, S.R.H., 1999, A comprehensive strategy for understanding flow in carbonate aquifers. In: Karst modeling, Eds. A.N. Palmer, M.V. Palmer and I.D. Sasowsky, Special Publication No. 5, Karst Waters Institute, Charles Town, WV, 30-37.

Worthington, S.R.H., 2001, Depth of conduit flow in unconfined carbonate aquifers, Geology, 29, 335-338.

Worthington, S.R.H., 2003, Numerical simulation of the Mammoth Cave aquifer, Kentucky. Geological Society of America Annual Meeting Abstracts.

Worthington, S.R.H., and D.C. Ford, 1997, Borehole tests for megascale channeling in carbonate aquifers. Proceedings of the 6th conference on limestone hydrology and fissured media. Centre of Hydrogeology, University of Neuchatel, 191-195.

Worthington, S.R.H., G.J. Davies, and D.C. Ford, 2000a, Matrix, fracture and channel components of storage and flow in a Paleozoic limestone aquifer. In: Groundwater flow and contaminant transport in carbonate aquifers, Eds. C. Wicks and I. Sasowsky, Balkema, Rotterdam, 113-128.

Worthington, S.R.H., D.C. Ford and P.A. Beddows, 2000b, Porosity and permeability enhancement in unconfined carbonate aquifers as a result of solution, in Speleogenesis: Evolution of karst aquifers, Eds. A. Klimchouk, D.C. Ford, A.N. Palmer and W. Dreybrodt, National Speleological Society, Huntsville, Alabama, p. 463-472.

Worthington, S.R.H., Schindel, G.M., and Alexander, E.C., Jr., 2002, Techniques for investigating the extent of karstification in the Edwards Aquifer, Texas. In: Hydrogeology and biology of post-Paleozoic carbonate aquifers, J.B. Martin, C.M. Wicks, I.D. Sasowsky (editors), Karst Waters Institute, Special Publication 7, p. 173-175.